

Dynamic responses of PCB under product-level free drop impact

Da Yu *, Jae B. Kwak, Seungbae Park, John Lee

Department of Mechanical Engineering, State University of New York at Binghamton, P.O. Box 6000, Binghamton, NY 13902, USA

ARTICLE INFO

Article history:

Received 20 November 2009

Received in revised form 7 February 2010

Available online 25 March 2010

ABSTRACT

The peak value of out-of-plane displacement of printed circuit board (PCB), when it is subjected to drop impact, is a major concern to electronic manufacturers as it relates to the maximum stress causing failure for the solder balls. In this work, the full-field dynamic responses of printed circuit boards (PCBs) of product level are measured and analyzed in detail with the aid of Digital Image Correlation (DIC) method. In contrast to the board level drop test, which can be more easily instrumented by following the JEDEC test standards, the product-level drop test requires great effort in controlling the impact orientation, which is critical to ensure the consistency of test results. Moreover, carefully guided free drop condition is essential in investigating the mechanical dynamic behaviors of PCBs to capture the realistic dynamic behaviors during free drop impact. Several effects of test variables, such as drop height, PCB supports, casing shape, and battery weight distribution, are carefully studied case by case. Along with the free drop impact experiments, the 3D FEA models are analyzed using ANSYS/LS-DYNA™. The simulation studies and experimental results are useful for improving the design of cellular phones with lower PCB deflection under impact shock.

Published by Elsevier Ltd.

1. Introduction

When portable electronic products are subject to impact shock, the solder ball stress level is the highest at the moment when PCB has the largest out-of-plane deformation with maximum bending stress, induced by the inertia force after impact [1]. Although the root cause of the package failure is the bending curvature between PCB and component [2], the out-of-plane deformation of PCB still provides us an insight into its dynamic responses under free drop impact. Especially when a cellular phone hits the ground horizontally, the out-of-plane deformation of PCB is the maximum among all other impact orientations. Therefore, investigations of dynamic responses of PCB under well-controlled free drop condition are important for the reliability assessment of cellular phone.

Board level drop test is much more conveniently conducted with instrumentation following the JEDEC test standards. Besides, the board level drop test is highly repeatable because of the fixed impact orientation. However, the board level drop test, which is also constrained drop test, may not represent the natural dynamic behaviors of electronic product under real drop impact condition. Because of the advantage of repeatability for the board level drop test over the product-level test, a large number of analytical and experimental researches have been preformed over the past few years [1–8], while relatively few work consider product-level drop impact.

Although the product-level free-drop test is complicated because consistency of experiment depends on many factors, such as drop height, product design, and especially the impact orientation, it is an important test as the PCB is subjected to more realistic drop condition compared with the board level drop test. For the first time, the full-field deformation of PCB during free drop impact has been characterized in this work.

During free-drop test, it is not feasible to mount sensors at any desired positions on the PCB because of its compact size; and the weight of sensors will dramatically change the dynamic responses of PCB, especially for the light electronic products, such as cellular phone. Cables from strain gages and accelerometers will undoubtedly affect the impact orientation leading to the inconsistency of experimental results.

In this work, a new approach of non-contact optical measurement is applied to investigate the dynamic responses of PCB under product-level drop test using Digital Image Correlation (DIC) method to produce a full-field deformation distribution of PCBs. In electronics package industry, DIC has been widely used to study the stresses in solder interconnects of BGA packages under thermal loading [10], and to study dynamic deformation for flexible bodies [11]. The possibility and applicability of DIC measurement in board level drop test of cellular phone have also been investigated [12–14]. With the help of DIC, product-level free-drop test is more feasible and controllable since perturbations from cables and the effects of sensors' weight have been eliminated.

In parallel with experimental studies, an accurately validated numerical model has been developed as an invaluable tool for

* Corresponding author. Tel.: +1 6073729167.

E-mail address: dyyu1@binghamton.edu (D. Yu).

analysis of the impact dynamic behavior and subsequent design optimization for PCB.

2. Experimental setup

A typical setup of product-level drop tester is shown in Fig. 1. The Lansmont® M23 was used in the free-drop test. PCBs of different shapes are mounted to the cellular phone case. The cellular phone case, which has four arms glued to two sides, rests on the flat-end slots of forks mounted on the top surface of shock table (230 mm × 230 mm). This pair of forks acts as a mean to hold cellular phone case during free drop. In the free-drop test, the shock table drops freely from a predefined height along the three guiding rods onto strike surface, which is placed on the top of seismic mass. As the shock table goes down, the cellular phone case hits the anvil (target surface) before the shock table hits the strike surface. This is important to avoid any vibration noise generated when the shock table hits the strike surface transmitting to the anvil during the free drop impact.

Repeatability of impact orientation is critical to measuring repeatable dynamic response. Small variations of the impact orientation can lead to huge difference in dynamic board responses [9]. Therefore, an adjustable pair of forks was developed for a repeatable free-drop system. The flat-end slots on the forks were made wider (5 mm) than the diameter of those arms (1 mm), which do not constrain any degree of freedom in X, Y, and Z direction when cellular phone hits the target surface. This design provides acceptable repeatability of initial position and desired impact orientation; and it allows cellular phone to rebound contact-free after impact and ensures the unconstrained behavior of PCB throughout the impact.

2.1. Digital Image Correlation with high-speed cameras

High-speed digital cameras have been set up to capture pictures of the board surface during impact frame by frame. Utilizing

advanced CMOS sensor technology, the high-speed cameras provide full mega pixel resolution (1024 × 1024-pixels) images at frame rate up to 3000 frames per second (fps), 512 × 512-pixels resolution at 10,000 fps and at reduced resolution to an unrivaled frame rate of 250,000 fps. As the pixel resolution and the size of field of view increase, the frame rate decreases. A proper frame rate (12,500 fps) is chosen in this work as having enough frame rate to capture the drop impact event while retain enough field of view.

Two halogen lighting provided the same light intensity for exposure time less than 10 μs. Pre- and Post-impact portions of the drop were extracted in the form of series of images. These images were then exported to ARAMIS for solving the full-field deformations, 3D profile, and the strain of PCB. Corners or sides of the PCB were chosen, depending on how PCB was mounted to the cellular phone case, as reference points for the purpose of 'movement correction' in ARAMIS to eliminate rigid-body motion.

Digital Image Correlation is a full-field optical measurement technique of which both the in-plane and out-of-plane deformations can be computed by comparing the pictures of the target object at initial and deformed stages. Thousands of unique correlation areas (known as subsets) are defined across the entire imaging area. These subset centers are tracked, in each successive pair of images, with accuracy of up to one hundredth of a pixel. Then, using the principles of photogrammetry, the coordinates of each facet are determined for each set of images. The results are the 3D surface profile of the component, the displacements, and the strains. Rigid-body motion can first be quantified and then removed to reveal relative deformations [12,13].

2.2. Test vehicle

The prototype cellular phone consists of a PCB and a case, which are assembled together with a rectangular frame and six screws (Figs. 2 and 4). In this investigation, PCBs, PCB1, 2, 3, 4, 5, and 6 (Table 1) are assembled with cellular phone cases, Cases 1, 2, 3,

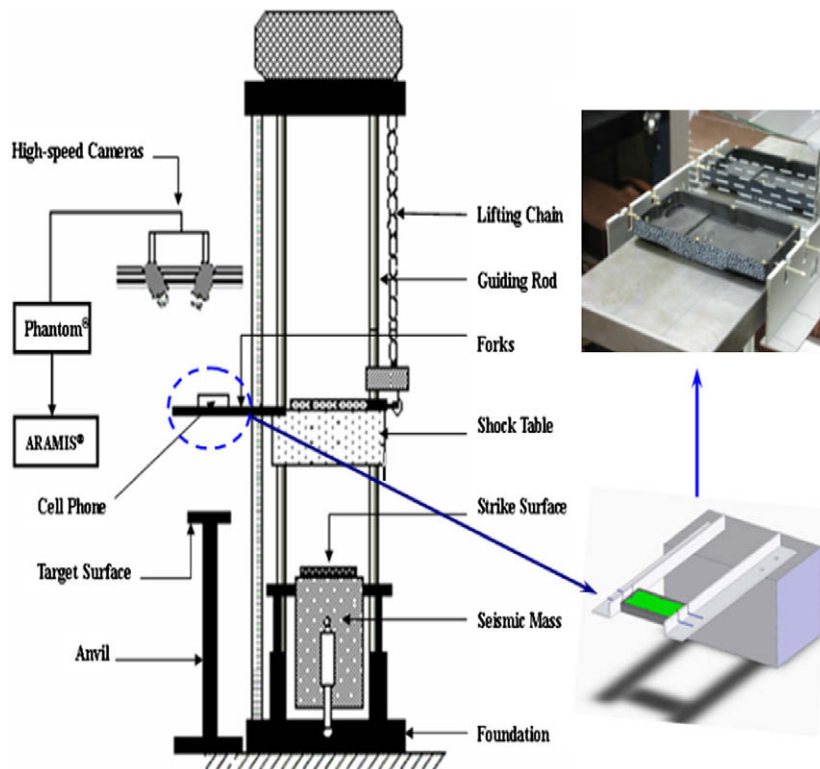


Fig. 1. Experimental setup: drop test facility and DIC measurement equipment.

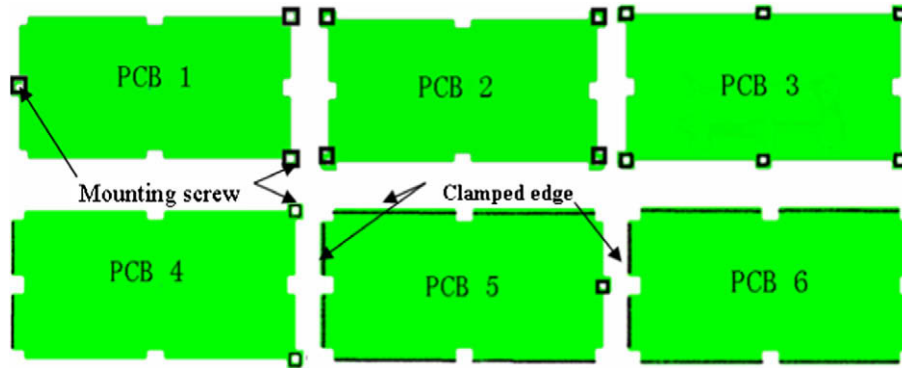


Fig. 2. Connecting configurations of PCB.

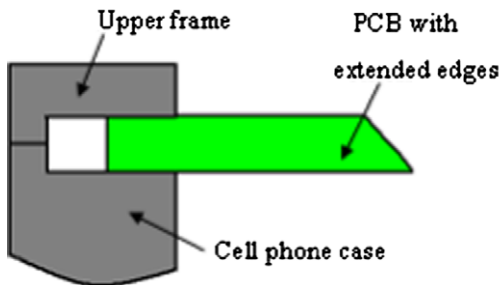


Fig. 3. PCB with extended edges clamped by upper frame and cell phone case.

and 4 (Fig. 4). PCB1, 2, and 3 are identical except in the number of mounting-tabs (with screw holes), three, four, and six tabs, respectively. They are secured to the casings only at the tabs by the frame screwed through the tab holes. PCB4, 5 and 6 have extended edges instead of tabs with screw holes. The same frames are used to clamp the PCBs along the extended edges with six screws as shown. Because of the extended edges the dimensions of PCB4, 5, and 6 are slightly different from PCB1, 2, and 3.

The four different case designs are named as Cases 1, 2, 3, and 4. All cases have the same length and width (106 mm × 56 mm) but

different bottom shapes, while the weight of each case is 25.8 g, 25.3 g, 24.8 g, and 23.8 g, respectively. The shape effects from the different contact dynamics are studied in this work. The walls are all identical in design and dimension with thickness of 2.48 mm. As noted, all PCBs are framed and clamped at the tabs or along the extended edges by six screws through the upper frame to the case wall.

2.3. Correlation of DIC data with accelerometer data

As a state-of-the-art measurement technique, Digital Image Correlation method integrated with high-speed cameras has unique advantages over traditional measurement: strain gages and accelerometers are no longer needed to obtain strain and acceleration at a certain point or even for a full field. This advantage is very important to free-drop test, especially for a compact-size electronic product.

Before performing free-drop tests with the aid of DIC measurement technique, a preliminary experiment was conducted to correlate results from Digital Image Correlation with accelerometer measurements taken simultaneously during the drop impact. The board acceleration is measured using Endevco accelerometer signal conditioner. Fig. 5 shows the top and bottom surfaces of the PCB. Acceleration levels of up to 10,000g can be accurately

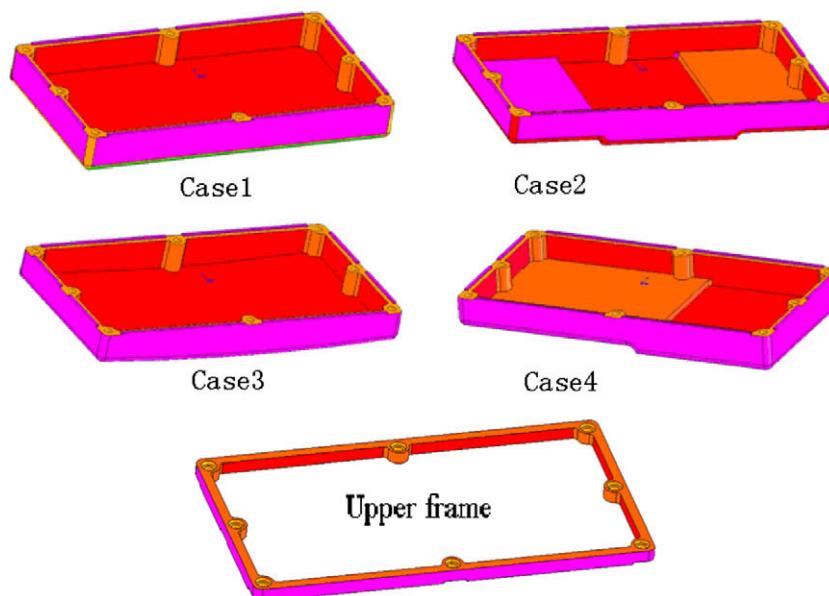


Fig. 4. Configurations upper frame and cellular phone cases.

Table 1

Dimension of PCB samples.

	Length (mm)	Width (mm)	Thickness (mm)
PCB1	106.0	56.0	1.0
PCB2	106.0	56.0	1.0
PCB3	106.0	56.0	1.0
PCB4	104.5	56.0	1.0
PCB5	104.5	53.0	1.0
PCB6	103.0	53.0	1.0

measured using a PE (piezoelectric) accelerometer. This accelerometer has a sensitivity of 0.608 pC/g with a weight of 0.45 g, which is 2.5% of the PCB. Ten inch drop height was chosen in order to satisfy the measurement range of accelerometer and to reduce the interference effects of wires on the dynamic response of PCB. Quadratic differentiation of digital data on out-of-plane displacement from DIC measurement provided the acceleration at the point where the accelerometer was mounted.

Since the data obtained from accelerometer contained high frequency noise, an appropriate low pass filter was necessarily applied before comparing these measurement results. Fig. 6 shows a good correlation between both measurements. This provided sufficient confidence on the current testing methodology and the DIC system.

2.4. Repeatability of free-drop tests

Impact orientation is one of the key factors affecting the dynamic responses of PCB. Repeatability of impact orientation is critical to guaranteeing a repeatable response.

To confirm the repeatability and controllability of impact orientation in the current experimental setup five drop tests were repeatedly performed. In these tests, the drop height was 20 in. and PCB was screw-mounted (PCB2) at four corners to the flat-bottom cellular phone case (Case 1). Fig. 7 shows the good repeatability of out-of-plane displacement, which is the deflection of PCB relative to the case. The variation of peak out-of-plane displacement was within ±2%. The results indicated that the measurement of PCB displacement was highly repeatable.

3. Free-drop test results

3.1. Effects of drop height

The PCB goes through a series of energy transformation during the drop event [3]. As cellular phone drops down with the drop table, the potential energy of PCB is converted into kinetic energy during the fall. When the cellular phone case hits the striking surface, the kinetic energy of PCB converts to strain energy in the form of downward bending under the inertia load. This uniformly

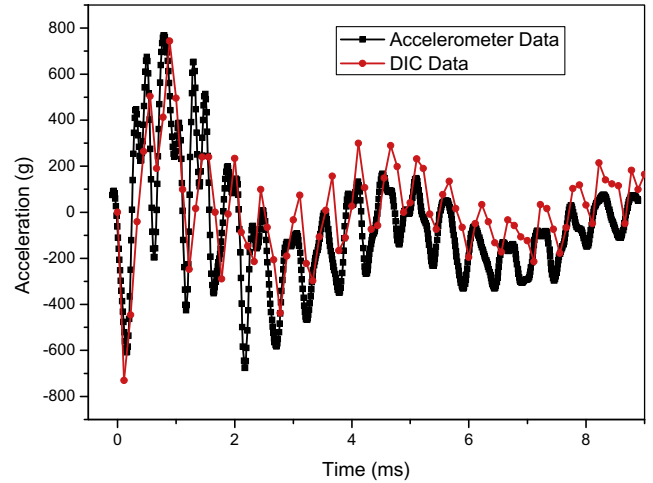


Fig. 6. Comparison of acceleration data: accelerometer (filtered) and DIC (calculated).

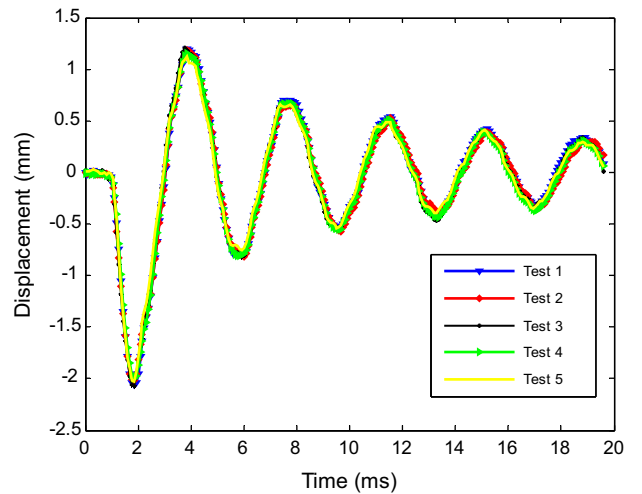


Fig. 7. Repeatability of out-of-plane displacement on PCB.

distributed inertia force is generated by the deceleration of the casing during the impact. With a uniform load, the PCB dynamics is dominated by the first mode of the flexural oscillation. At the maximum bending, the energy exchange is reversed and PCB undergoes the damped flexural oscillation. Thereafter, the PCB bends up and down cyclically, while the phone case moves interacting with PCB, until it fully damps out due to the energy dissipation mostly through the frictions in mounting-screws and clamped-edges.

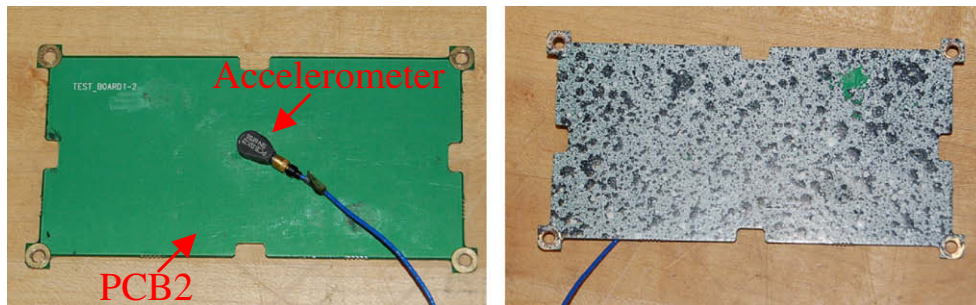


Fig. 5. The attachment of accelerometer on PCB.

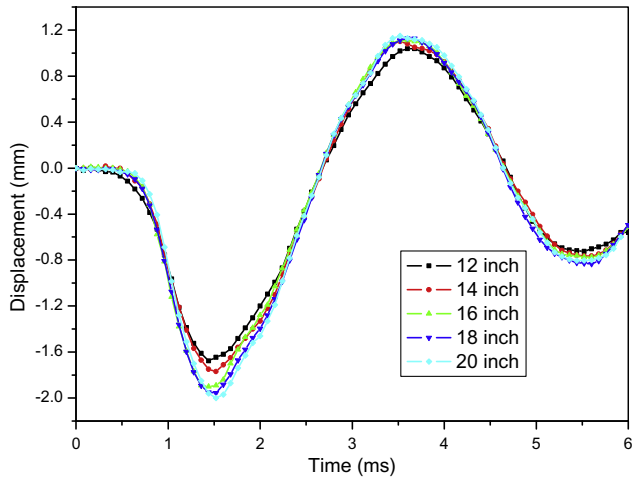


Fig. 8. Out-of-plane displacement of Case 1 PCB2 under different drop height.

The amount of potential energy of PCB, which will be transformed to kinetic energy and then finally be converted to the inertial load applied to the PCB, is determined by the drop height. Thus, the drop height highly affects the maximum out-of-plane displacement of PCB, which is approximately proportional to the square root of the drop height. Since the natural frequencies and mode shapes are structure dependent, the drop height, which acts as the external load on PCB, does not affect the bending mode or frequency of its dynamic response.

In this test, the flat-bottom cellular phone case (Case 1) with four-corner screw-mounted PCB (PCB2) was dropped from a height of 12, 14, 16, 18, and 20 in. Fig. 8 shows the out-of-plane displacement at the PCB center, where the displacement is the maximum, under different drop height conditions.

3.2. Effects of mounting-screw

Position and number of mounting-screws connecting PCB with the cellular phone case are crucial to the PCB bending modes and

its dynamic response. In this test, three different connecting configurations are selected and analyzed under the same drop conditions: all PCBs are connected to the flat-bottom cellular phone case (Case 1) and dropped from 20 in. height.

The bending mode shape depends on the connecting configurations (boundary conditions). PCB with four points screwed to cellular phone case (PCB2), due to its symmetry, has the maximum displacement (2.04 mm) at the PCB center as shown in Table 2. PCB with three mounting-screws (PCB1) has similar mode shape as PCB2's, but at lower frequency due to the reduced constraint. However, the maximum displacement (2.15 mm) is slightly shifted to points 2 and 3 of PCB1, as shown in Table 2. PCB3, which is screwed to the case with two additional screws, has totally different bending shape compared with PCB1 and PCB2, and has two symmetrical maximum out-of-plane displacements (0.53 mm) at points 2 and 3. Compared with the PCB2, the amplitude of PCB3 was significantly reduced, due to the change in boundary conditions. More constraint was applied with two additional mounting-screws to PCB, reducing the bending down behavior of PCB and changing its bending shape. The frequencies of three cases are different. As shown in Table 2, the PCB3 has the highest frequency (735 Hz), followed by the PCB2 (260 Hz), and the PCB1 (225 Hz). Although the frequency difference can be explained in terms of constraints, the amplitudes cannot be related to the constraints alone. It is related to the dynamic response of the phone case to the striking surface, that is, the pulse profile of the inertia load dictates the PCB amplitudes (see Fig. 9).

3.3. Effects of clamped-edge

In addition to the mounting-screw method, the clamping method is also used to attach PCBs (PCB4, 5, and 6, Fig. 2) to the case, and their effects on dynamic responses were investigated. The same drop condition (cellular phone case and drop height) was applied in this test. The results are summarized in Table 2.

PCB4 has the same bending mode as PCB2, which approximates the conditions of a clamped-clamped plate. Therefore, both cases

Table 2 Dynamic responses of different PCB.

Test vehicles	First bending mode	Max. displacement and frequency
<p>PCB1</p>		2.15 mm, 225 Hz
<p>PCB2</p>		2.04 mm, 260 Hz
<p>PCB3</p>		0.53 mm, 735 Hz
<p>PCB4</p>		2.13 mm, 223 Hz
<p>PCB5</p>		0.61 mm, 893 Hz
<p>PCB6</p>		0.64 mm, 833 Hz

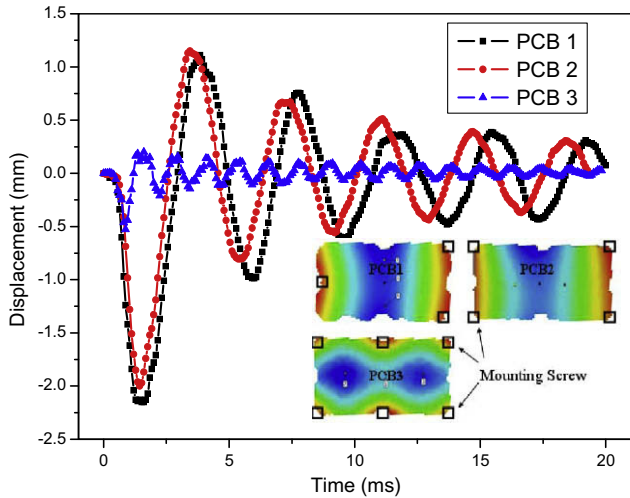


Fig. 9. Out-of-plane displacement for different PCBs.

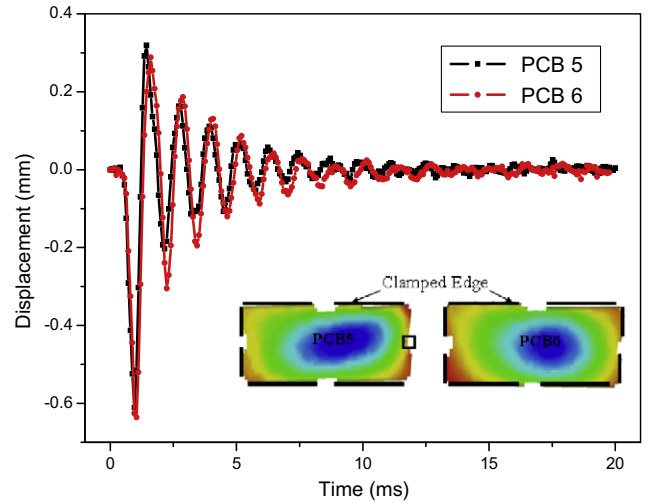


Fig. 11. Out-of-plane displacement for PCB5 and 6.

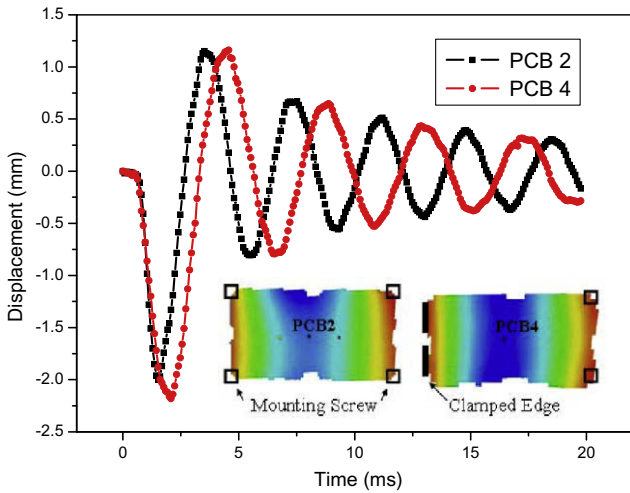


Fig. 10. Out-of-plane displacement for PCB2 and PCB4.

have the maximum out-of-plane displacement at the center of PCB. However, the first negative displacement peak of PCB4 is larger than PCB2 while the following peaks are slightly smaller (Fig. 10). The oscillation frequency of PCB4 is lower than PCB2's, indicating that the clamping used for PCB4 provided lower constraint than the tab connection for PCB2. Also, the decaying rate of PCB4 amplitude was faster. Since the only difference between PCB4 and PCB2, was the connection method, it can be concluded that, contrary to the appearance, the tab connection has provided higher constraint but lower damping. As clearly shown in Fig. 3, PCB4, which is clamped between upper frame and cell phone case, can slide along the clamped areas during its oscillation process after impact, and therefore less constraint is provided by clamping connection.

Bending modes of PCB5 and PCB6 are totally different from PCB2 and PCB4 as expected from the additional constraints on side edges. However, Figs. 10 and 11 again show that the dynamic responses die out much faster for PCB5 and 6 (within 14 ms) than for PCB2 or PCB4, owing to the clamped-edges.

In summary, the test showed that clamped-edge resulted in a higher damping compared with mounting-screw, indicating more energy dissipated through the clamped-edge than the mounting-screw. Also, more constraint is applied to the PCB through mounting-screw than the clamped-edge.

3.4. Effects of casing shape

Casing shape affects the impact velocity and the acceleration loading applied to the PCB during impact. Those parameters have influence on the dynamic behavior of PCB. In this experiment, the same PCB (PCB2) are assembled to four different shape cell phone cases and dropped from 20 in. high. Cases 1, 2, and 3 are all symmetric lengthwise about the central line providing symmetric loading to PCB.

When the cell phone cases were dropped from 20 in. high with speckle patterns marked on their sidewall, high-speed cameras were placed to capture the sidewall of cell phone case. Displacement data of the sidewall without "rigid-body movement correction" can be extracted from ARAMIS®. The average of five points' displacement response data represented the overall movement of the cell phone case during impact. Velocity right before and after impact (Table 3) can be determined from the slopes of the displacement response curve.



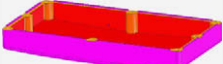

Fig. 12 indicates Case 3, which has curved bottom surface, has the largest out-of-plane displacement (2.64 mm), followed by Case 2 (2.44 mm), and Case 1 (2.04 mm). According to Table 3 on impact velocities, the Case 1 has the lowest velocity before impact (v_{impact}). Therefore, it can be argued that the least kinetic energy of PCB, which causes the bending down of PCB, is converted into inertial load. That is, depending on the casing shape, different amount of energy, which is in form of acceleration loading, is applied to the PCB during impact. For flat bottom surface case, it has the largest energy loss during the impact event (according to Table 3), and thus, the least energy is transmitted to PCB. As a result, Case 1 has the smallest amplitudes of the out-of-plane displacement.

Case 4, which is asymmetric about its center, hits the striking surface twice. The right part of cell phone case (Fig. 4) hits first, followed by the left part. The double impact leads to a complex response shown in Fig. 12: the response caused by the inertia load from the first impact is superimposed by the response to the second impact.

3.5. Effects of battery weight distribution

This part of work is to investigate the influence of battery distribution on the dynamic response of PCB, because in real situation a battery is always attached to the cell phone case. In this test, one battery (40 mm × 36 mm × 6 mm, 18.6 g) was attached

Table 3
Velocity measurement results.

Cellular phone case	Contact area size (mm)	Velocity before and after rebound (mm/s)
	106 × 56	$v_{\text{impact}} = 2430, v_{\text{rebound}} = 278$
	44 × 56	$v_{\text{impact}} = 2511, v_{\text{rebound}} = 986$
	N/A × 56	$v_{\text{impact}} = 2674, v_{\text{rebound}} = 2065$
	46 × 56	$v_{\text{impact}} = 2509, v_{\text{rebound}} = 928$

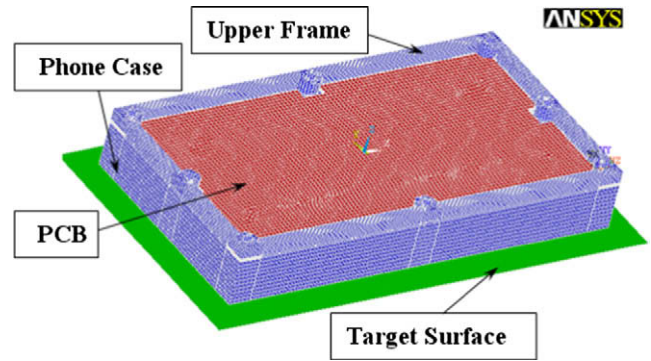


Fig. 15. A 3D finite element model of the cellular phone assembly.

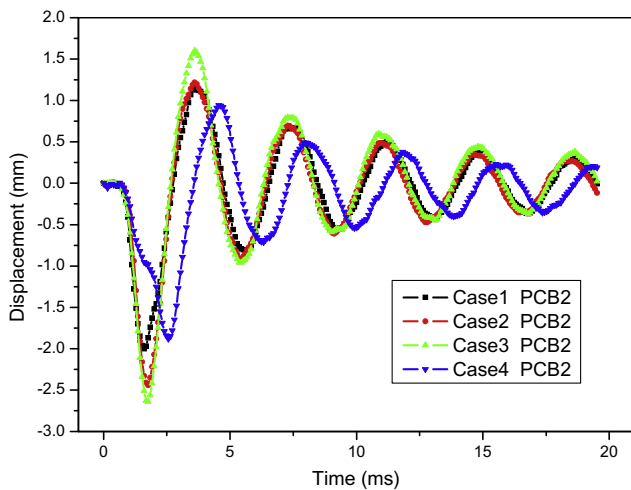


Fig. 12. Out-of-plane displacement for different case.



Fig. 13. Battery located at left and center of cell phone case.

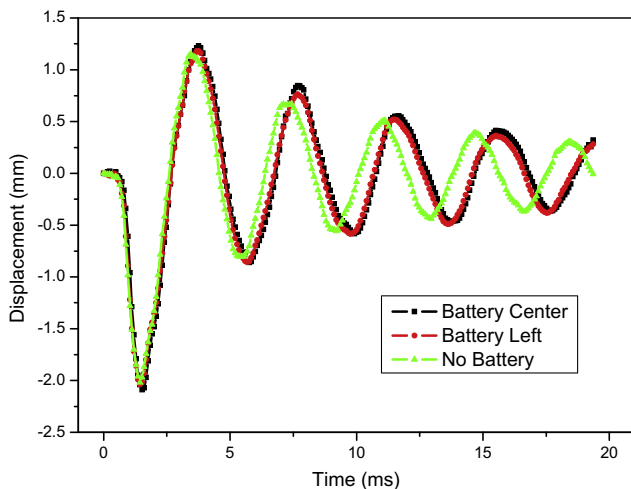


Fig. 14. Out-of-plane displacement for battery distribution effect.

to different location of flat-bottom phone case (Case 1) with PCB2 mounted on it (Fig. 13). The cell phone together with battery was dropped from 20 in. height.

The dynamic responses of PCB are greatly affected by the impact orientation. Since the experiment setup can provide close-to-ideal impact orientation with good repeatability, the battery distribution has little influence on the impact orientation. Thus, Fig. 14 indicates that the responses of PCB for battery located at left and center are almost the same (both amplitude and frequency). The added mass of battery weight merely affects the frequency of dynamic response. Cellular phone without battery has higher frequency as shown in Fig. 14.

4. Numerical modeling and results

ANSYS/LS-DYNA have been used to develop a numerical model for the product-level free-drop test. The focus of this numerical model is to simulate dynamic responses of PCB under free drop impact and verify experimental results.

4.1. Finite element model

In contrast to the board-level drop simulation, which applies the input-G method [15], the product-level drop simulation is more complicated as both phone casing and PCB should be modeled in detail. Fig. 15 shows a 3D finite element model of the cellular phone assembly in this work. The assembly consists of a phone case, PCB, and an upper frame, which were modeled mainly using hexahedral SOLID164 element.

Linear elasticity material models were considered in this work. All the material properties listed in Table 4 were obtained through measurements treating as isotropic. Even PCB is considered isotropic. As shown in one reference, which deals with a finite element analysis intended to describe numerically the behavior of multi-layered PCB model in the drop-impact performance, the PCB is modeled as isotropic, orthotropic and multi-layer fill-warp. Through the comparison of experimental results, the error of displacement amplitude of those models decreases from 9.41%, 8.62%, to 1.18%. However, the CPU times increase from 18 min 48 s, 22 min 56 s, to 2 h 29 min 41 s [16]. Therefore, isotropic model has the highest computational efficiency and reasonable accuracy of model among those models.

Accurate modeling of contact interfaces between bodies is crucial to the prediction capability of the finite element models. Contact surfaces in LS-DYNA allow the user to represent a wide range of interaction between components in a model [17]. The treatment of impact along interfaces has always been an important capability in LS-DYNA.

Interfaces can be defined by listing in arbitrary order all triangular and quadrilateral segments that comprise each side of the interface. One side of the interface is designated as the slave side, and the other is designated as the master side. Nodes lying in those

Table 4
Material properties.

Materials	Model	Young's modulus (GPa)	Poisson ratio (ν)	Density (kg/m ³)
PCB	Isotropic	25.0	0.35	3380
Case and upper frame	Isotropic	2.1	0.40	1160
Target surface	Isotropic	210.0	0.34	7800

surfaces are referred as the slave and master nodes respectively. In LS-DYNA, a contact is defined by identifying (via parts, part sets, segment sets, and/or node sets) what locations are to be checked for potential penetration of a slave node through a master segment. A search for penetrations, using any of a number of different algorithms, is made every time step.

Tied contact “glue” the slaves to the masters. The slave node is forced to maintain its isoparametric position with the master segment. The effect is that the master segments can deform and the slave nodes are forced to follow that deformation [17]. Therefore, tied surface to surface (TDSS) contact together with automatic surface to surface (ASTS) contact was applied to couple different phone assembly parts.

ASTS contact was also used to define contact between the bottom of phone case and the target surface (steel plate), which was modeled as a rigid surface.

4.2. Damping parameters

Random vibration test is chosen to characterize the damping ratio, since it excites multiple natural frequencies in one sweep [18]. The experimental setup consisted of a Dynamic Systems Shaker. The test vehicles were screwed to four standoffs as shown in Fig. 16. Two accelerometers were used to characterize the system; one accelerometer was placed on the shaker fixture to measure the input acceleration to the system, G_{in} , and the second accelerometer was placed on top of the PCB to measure the output acceleration, G_{out} .

From Fig. 17, it is also possible to determine the damping ratio of the single mass-spring system using Eq. (1) [19]

$$\xi = \frac{\Delta f}{2f_n} \quad (1)$$

where Δf is the bandwidth of the half power points. These half power points are frequencies where the response is $1/\sqrt{2}$ or 0.707 of its peak value. Using $f_n = 266$ Hz and $\Delta f = 5$ Hz, the damping ratio ξ is found to be 0.0094.

In ANSYS/LS-DYNA, Rayleigh damping, the only type of damping for transient analysis, is a linear combination of alpha and beta damping (Eq. (2)).

$$[C] = \alpha \times [M] + \beta \times [K] \quad (2)$$

where C , M , and K are damping, mass and stiffness matrices respectively.

Alpha damping, known as mass proportional damping, is intended to damp rigid-body motion, while beta damping mainly affects higher-frequency motion. Beta damping is orthogonal to rigid-body motion, therefore has little effect on damping out this behavior [20].

Alpha and beta damping can be estimated from damping ratio ξ using the following relationship known for the mass-spring model with natural frequencies, ω_1 and ω_2 :

$$\xi = \frac{\alpha}{2\omega_1} + \frac{\beta\omega_1}{2} = \frac{\alpha}{2\omega_2} + \frac{\beta\omega_2}{2} \quad (3)$$

Since a uniform load is applied to the PCB during the downward bending, the PCB dynamics is dominated by the first mode of the

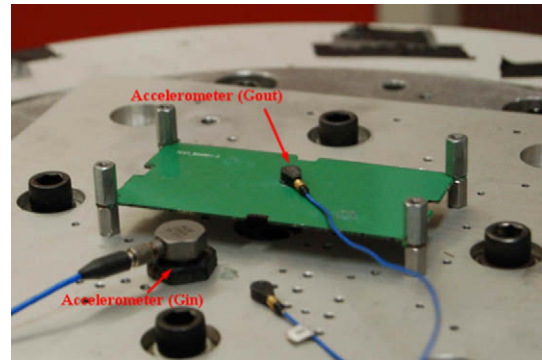


Fig. 16. Experimental setup for random vibration test.

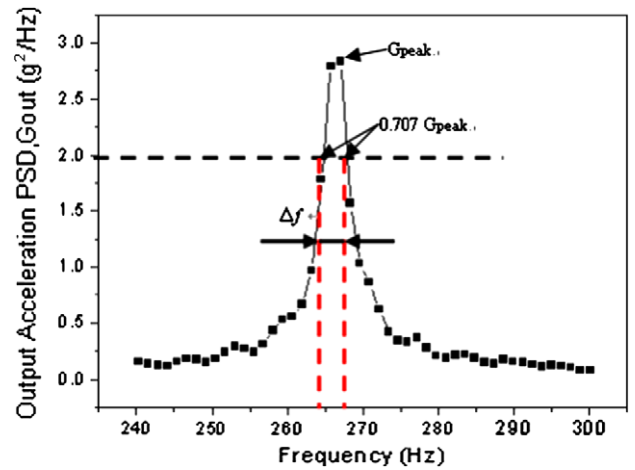


Fig. 17. Vibration test result to determine the damping ratio.

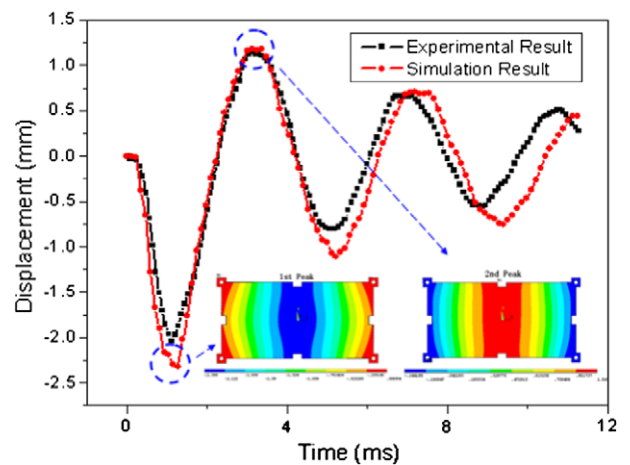


Fig. 18. Out-of-plane displacement at the center of PCB2 with four mounting-screws to the bottom case.

flexural oscillation. Assuming the first mode ($\omega_1 = 258.2$ Hz) and the fourth mode ($\omega_2 = 1174.3$ Hz) to cover the full range of frequencies that could be excited during the free-drop test, Eq. (3) yields $\alpha = 25$ and $\beta = 1.3e-5$.

4.3. Initial conditions and loading

In free drop simulation, only acceleration and initial velocity are considered as loading for the transient dynamics analysis. To save

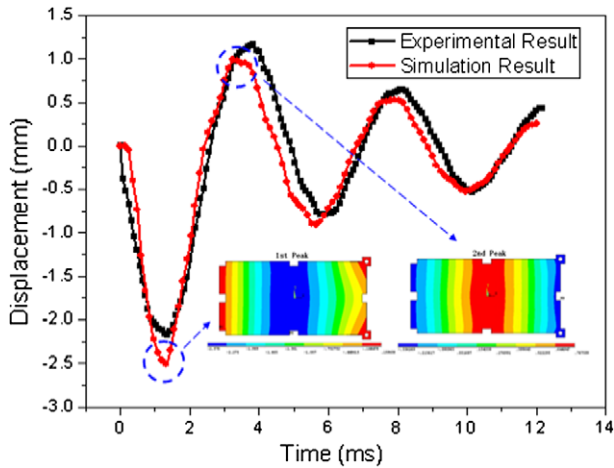


Fig. 19. Out-of-plane displacement at the center of PCB4 with one clamped-edge and two mounting-screws.

Table 5
Comparison between simulation and experimental results.

	Magnitude of the first peak (mm)		Frequency (Hz)	
	Simulation	Experiment	Simulation	Experiment
PCB2	-2.32	-2.04	247	260
PCB4	-2.50	-2.18	232	223

computational time, the velocity right before impact was applied as an initial condition. In the absence of air drag, the theoretical impact velocity for free drop of height, h , and gravitation, g , is:

$$V = \sqrt{2gh} \quad (4)$$

Actual impact velocity (as listed in Table 3 is around 2500 mm/s) measured by high-speed cameras is smaller than theoretical calculated velocity (3155 mm/s). In the most part of drop, the velocity loss comes from two parts. First, one part of velocity loss is due to friction between drop table and guiding rods during drop test. This effect can not be totally eliminated. However, it can be minimized by regular lubrication on guiding rods. Second, there is air drag. This also cannot be eliminated. There is also an additional deceleration

for cellular phone near the impact surface beginning from about 1 mm above the target surface owing to air cushion between the bottom surface and the target surface. This can be significant if the impact surfaces are very smooth as it also dissipates significant amount of energy. For rough or irregular surfaces air cushion is negligible. In simulation model, although friction effect and air cushion effect were not specifically considered, energy loss due to those effects was taken into account by applying measured velocity instead of theoretical calculated velocity. The velocity correction is necessary and justified for realistic results in view of the consistency in measured data on the friction effect and air cushion effect as shown in previous work [18].

4.4. Simulation results

The developed numerical model was validated by comparing the displacement at the center of the PCB and the vibration frequency for both PCB2 and PCB4 assembled with the flat-bottom cellular phone case (Case 1) with the experimental results.

Figs. 18 and 19 show good agreement between the simulation and experimental results. The vibration frequency and phase for both simulation and experiment match each other closely. However, the simulation seems to over predict the out-of-plane displacement especially for the first peak. A summary of result correlation is found in Table 5. The percent errors of the first displacement peak between the simulation and experiment are 14% (PCB2) and 15% (PCB4). The percent errors of frequency are 5% and 4%, respectively.

The full-field deformation distribution contour plots can be readily extracted from ANSYS/LS-DYNA to further validate the experimental results. Figs. 20a and 20b shows these contour plots at the time of first and second peaks after drop impact together with snapshots from DIC taken at the same time. Good agreement between the simulation and experiment was observed. Figs. 20a and 20b clearly shows that the simulation captured the dynamic responses of PCB almost entirely, by predicting not only the time-history of the peaks but also the location of the maximum and minimum peaks. The small difference between the simulation and the experiment is believed to be due to some experimental errors such as slight impact angle deviation of PCB at the moment of impact.

Fig. 21 shows the effect of clamped-edge on the deformation of PCB in the simulation. It clearly indicates that PCB4 has a larger

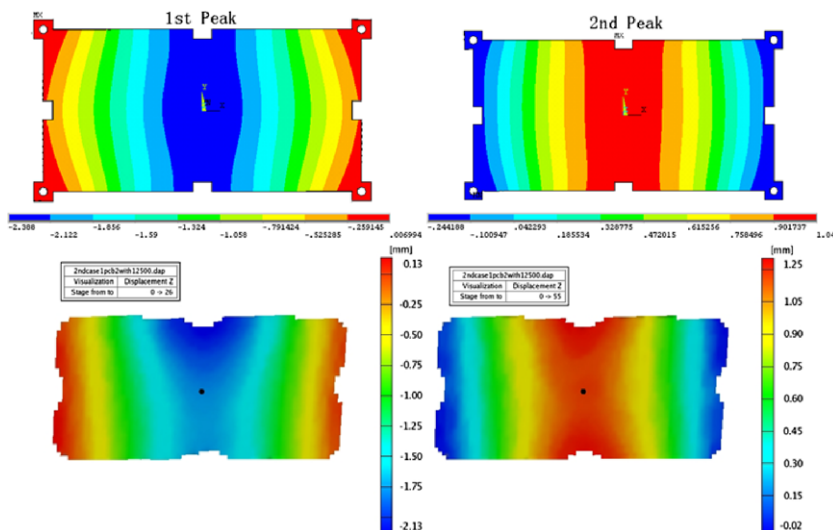


Fig. 20a. Out-of-plane displacement contour plots for PCB2 from simulation and experiment.

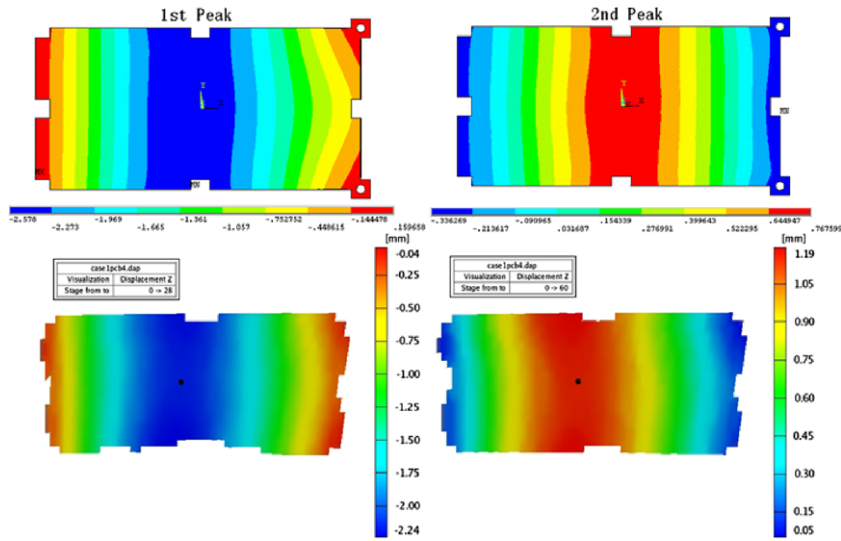


Fig. 20b. Out-of-plane displacement for PCB4 from simulation and experiment.

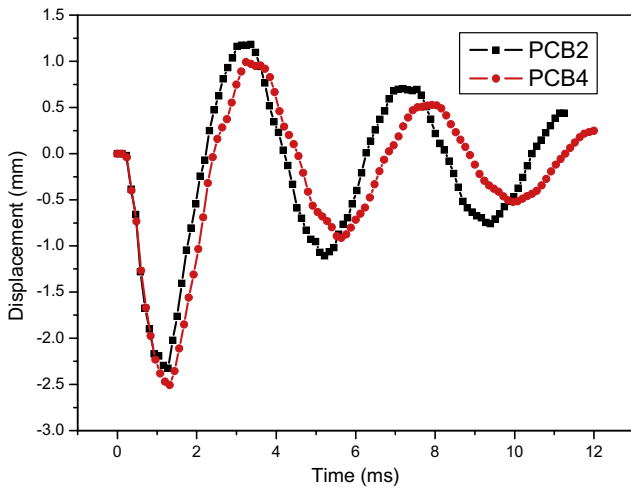


Fig. 21. Out-of-plane displacement for PCB2 and PCB4 in simulation.

first negative displacement peak (2.50 mm). However, the subsequent peaks and frequency (232 Hz) are smaller than PCB2's. This trend is also validated with the experimental results and the reason is explained in detail in previous section (Fig. 10).

5. Discussions

Both of experimental and simulation results indicate that the out-of-plane displacement dramatically decreases with applying more constraints to the PCB. In this regard PCB6, all of whose sides are fixed between the upper and lower cases, is found to be the best with the lowest out-of-plane displacement and best damping characteristics.

The over prediction of the first two peak displacement in the simulation can be explained by unknown damping parameters such as material damping (α) and structural damping (β) in the numerical model. The use of linear elastic material models for all parts, which will lead to a perfect impact condition without any energy loss, has also some considerable contribution to the over prediction.

Two damping parameters (α and β) will be measured and then the effects on impact behaviors will be investigated. In addition,

energy loss in the system will be studied and included in the model.

The PCB and cell phone case coupling, which was realized by the “Tied contact”, seems to be a good representation of the screw and surface coupling in experiment as indicated by the good agreement of vibration phase between simulation and experiment.

6. Conclusions

A new methodology of deformation measurement using high-speed cameras integrated with Digital Image Correlation technique has been used to analyze the dynamic responses of PCB under free drop conditions. Acceleration data obtained from the Digital Image Correlation technique is in good agreement with those obtained by using accelerometer. Great effort was made to control the impact orientation, which is crucial to ensure the consistency of test results for product-level free-drop test. Good repeatability of deformation measurement is shown in the experimental results.

Different PCB-phone case assembly methods were considered and the impact response for each case has been assessed respectively. The change of boundary condition of PCB will lead to different dynamic responses and bending mode shapes for PCB. In general, as the number of mounting-screw increase, more constraint is applied to the PCB and the maximum out-of-plane displacement decreases. The presence of clamped-edge results in higher damping compared with mounting-screw. However, more constraint is resulted to the PCB through mounting-screw than the clamped-edge. Casing shape affects both the maximum deformation and impact velocity. The curved bottom phone case has the largest out-of-plane displacement while the flat-bottom phone case has the minimum.

Both out-of-plane displacement and vibration frequency of PCB, obtained from this model, show good agreement with the DIC measurements. Presently, further improvement of the model is being investigated, and a better agreement with measurement is expected to be achieved.

Acknowledgments

This work was partially supported by Samsung Electronics and IEEC of State University of New York at Binghamton. The authors appreciate the financial support.

References

- [1] Kim JG, Park YK. Experimental verification of drop/impact simulation for a cellular phone. *Exp Mech* 2004;44(4):375–80.
- [2] Gu Jie, Lim CT. Modeling of solder joint failure due to PCB bending during drop impact. In: Proceedings of the 6th electronic packaging technology conference, EPTC, Singapore; 2004. p. 678–83.
- [3] Luan JE, Tee TY. Novel board level drop test simulation using implicit transient analysis with Input-G method. In: Proceedings of the 6th electronic packaging technology conference, EPTC, Singapore; 2004. p. 671–7.
- [4] Tee Tong Yan, Ng Hun Shen, Lim Chwee Teck, Pek Eric, Zhong Zhaowei. Impact life prediction modeling of TFBGA packages under board level drop test. *Microelectron Reliab* 2004;44:1131–42.
- [5] Chai TC, Sharon Quek, Hnin WY, Wong EH. Board level drop test reliability of IC packages. In: Proceedings of the 55th electronic components and technology conference, ECTC, Lake Buena Vista, FL; 2005. p. 630–36.
- [6] Wong EH, Mai Y-W. New insights into board level drop impact. *Microelectron Reliab* 2006;46(5–6):930–8.
- [7] Qu Xin, Chen Zhaoyi, Qi Bo, Lee Taekoo, Wang Jiaji. Board level drop test and simulation of leaded and lead-free BGA-PCB assembly. *Microelectron Reliab* 2007;47(12):2197–204.
- [8] Ong YC, Shim VPW, Chai TC, Lim CT. Comparison of mechanical response of PCBs subjected to product-level and board-level drop impact tests. In: Proceedings of the 5th electronic packaging technology conference, EPTC, Singapore; 2003. p. 223–7.
- [9] Wang HL et al. Drop tester with orientation repeatability for electronic products. *Exp Tech* 2006.
- [10] Zhou P, Goodson KE. Sub-pixel displacement and deformation gradient measurement using digital image-speckle correlation (DISC). *Opt Eng* 2001;40(8):1613–20.
- [11] Yogel D, Grosser V, Schubert A, Michel B. MicroDAC strain measurement for electronics packaging structures. *Opt Las Eng* 2001;36:195–211.
- [12] Park Seungbae, Shah Chirag, Kwak Jae B, Jang Changsoo, Chung Soonwan, Pitarresi James M. Measurement of transient dynamic response of circuit boards of a hand-held device during drop using 3D digital image correlation. *J Electron Packag* 2008;130(4):0445021–23.
- [13] Park Seungbae, Shah Chirag, Kwak Jae, Jang Changsoo, Pitarresi James, Park Taesang et al. Transient dynamic simulation and full-field test validation for a slim-PCB of mobile phone under drop/impact. In: Proceedings of the 57th electronic components and technology conference, ECTC, Reno, Nevada; 2007. p. 914–23.
- [14] Lall Pradeep, Panchagade Dhananjay, Iyengar Deepti. High speed digital image correlation for transient-shock reliability of electronics. In: Proceedings of the 57th electronic components and technology conference, ECTC, Reno, Nevada; 2007. p. 924–39.
- [15] Tee TY, Luan JE, Pek E, Lim CT, Zhong Z. Advanced experimental and simulation techniques for analysis of dynamic responses during drop impact. In: Proceedings of the 54th electronic components and technology conference, ECTC, Las Vegas, NV; 2004. p. 1088–94.
- [16] Yuqi Wang et al. Modeling and simulation for a drop-impact analysis of multi-layered printed circuit boards. *Microelectron Reliab* 2006;46:558–73.
- [17] LS-DYNA users guide.
- [18] Park Seungbae, Da Yu, Al-Yafawi Abdullah, Kwak Jae, Lee John. Effect of damping and air cushion on dynamic responses of pcb under product level free drop impact. In: Proceedings of the 59th electronic components and technology conference, ECTC, San Diego (CA); 2009. p. 1256–62.
- [19] Ginsberg JH. Mechanical and structural vibrations theory and applications. 1st ed. New York: Wiley; 2001.
- [20] ANSYS, Inc. ANSYS[®] v11.0. Theory manual.